DOI 10.1007/s11182-016-0728-5

Russian Physics Journal, Vol. 58, No. 12, April, 2016 (Russian Original No. 12, December, 2015)

SPATIOTEMPORAL DYNAMICS OF THE WIND VELOCITY FROM MINISODAR MEASUREMENT DATA

V. A. Simakhin,[1] O. S. Cherepanov,[1] and L. G. Shamanaeva[2,3] UDC 551.596; 53.082.4

The spatiotemporal dynamics of the three wind velocity components in the atmospheric boundary layer is analyzed on the basis of Doppler minisodar measurements. The data were processed and analyzed with the help of robust nonparametric methods based on the weighted maximum likelihood method and classical methods. Distribution laws were obtained for each wind velocity component. There are outliers in the distribution functions; both right and left asymmetry of the distributions are observed. For the x- and y-components, the width of the distribution increases as the observation altitude is increased, but the maximum of the distribution function decreases, which is in agreement with the data available in the literature. For the z-components the width of the distribution remains practically constant, but the value of the maximum also decreases with altitude. Analysis of the hourly semidiurnal dynamics showed that all three components have maxima in the morning and evening hours. For the y- and z-components the maxima in the evening hours are more strongly expressed than in the morning hours. For the x- and y-components the horizontal wind shear is closely tracked in the evening hours. It is shown that adaptive estimates on the efficiency significantly exceed the classical parametric estimates and allow one to analyze the spatiotemporal dynamics of the wind velocity, and reveal jets and detect wind shears.

Keywords: acoustic sounding, estimates of the weighted maximum likelihood method, robust nonparametric estimates, spatiotemporal dynamics of the wind velocity.

INTRODUCTION

Information about the spatiotemporal dynamics of the wind velocity, its mean value, variance, and structure functions in the atmospheric boundary layer (ABL) is of both fundamental and applied significance. It is needed to study the dynamics of atmospheric processes, to predict the state of the air basin, to estimate pollutant transport, to construct models of the ABL, to make weather forecasts, and to ensure safety of takeoff and landing of aircraft. Doppler acoustic radars (sodars) allow one to obtain the three wind velocity components with high spatial (down to several meters) and temporal (from 1 to 30 min) resolution and to analyze their spatiotemporal dynamics [1, 2]. The distribution law of the the wind velocity components is in general unknown, and various parametric models are used to describe it. Thus, Breadly [2] used a Gaussian and a parabolic shape of the distribution. Rykhlov [3] observed that the Weibull distribution model possesses a number of advantages over the more often used normal, lognormal, and Maxwellian model distribution laws for the wind velocity. For an unknown distribution law these models can give an inadequate description of the observed distribution of the wind velocity. What is more, the signal has random outliers. Processing of moderate-sized files of wind velocity data from meteorological masts allowed us in the manual curve-fitting mode to use standard methods to process the data. Large data files obtained by sodars require the creation of automated data

[1]Kurgan State University, Kurgan, Russia, e-mail: sva_full@mail.ru; ocherepanov@inbox.ru; [2]V. E. Zuev Institute of Atmospheric Optics of the Siberian Branch of the Russian Academy of Sciences, Tomsk, Russia, e-mail: sima@iao.ru; [3]National Research Tomsk State University, Tomsk, Russia. Translated from Izvestiya Vysshikh Uchebnykh Zavedenii, Fizika, No. 12, pp. 176–181, December, 2015. Original article submitted June 15, 2015.

processing systems, including online operation employing processing and analysis methods based on robust nonparametric statistics [4–7].

This article investigates special features of the spatiotemporal dynamics of the wind velocity extracted from real-time measurements obtained using a Doppler minisodar, and an analysis and comparison of standard classical methods with methods based on robust nonparametric statistics are carried out.

1. STATEMENT OF THE PROBLEM

We investigate the spatiotemporal dynamics of the three wind velocity components in the ABL on the basis of Doppler sodar measurements made using an AV4000 minisodar with a 50-element phase antenna array [8]. The working frequency of the minisodar was 4900 Hz, pulse duration 60 ms, and acoustic radiation was emitted sequentially in three directions – vertically and at angles $\alpha = 18°$ with respect to the vertical in two mutually orthogonal planes. The pulse repetition period was 4 s. Measurements were made at 40 altitude strobes z_j with resolution $\Delta z = 5$ m in the altitude range 5–200 m. Series of $N = 150$ profiles each were processed, which ensured averaging over a 10-minute measurement period. The measurements were carried out over the course of six (6) days in autumn from 12 to 17 September. Results of processing of the minisodar data for the three wind velocity components on the basis of the least squares method (LSM) are presented in [9–11]. A parametric model of the vertical profile of the horizontal wind velocity was constructed for neutral and unstable stratifications of the atmosphere. The spatiotemporal dynamics of the *x*-, *y*-, and *z*-components of the wind velocity was analyzed.

The random vector of the components of wind velocity $\boldsymbol{V}(t,z) = (V_x, V_y, V_z)$ depends on the time t of the measurement and on the altitude z above the underlying surface and forms a random process that depends on the parameter z (a random wind field). The random vector was defined by a number of n-dimensional distributions dependent on a large number of factors such as location, the underlying surface, time, altitude of the measurement, etc. It is obvious that to construct a mathematical model of the wind velocity in the ABL on the basis of such n-dimensional distributions (models of which are lacking) would be extraordinarily complex if even possible. Therefore the problem is decomposed into a sequence of simpler problems, on the basis of which particular mathematical models are constructed and solutions are extracted. Stable factors are assigned fixed values – location, the underlying surface, time and altitude of the measurement, and the following problems are considered:

1. Synthesis and analysis of strobe array (cell array). The time $t = t_0$ and altitude $z = z_0$ are assigned and the cell $\boldsymbol{V}(t_0, z_0)$ is singled out. Models of marginal cell distributions, parameters of position (average value), scale (variance), and confidence intervals are introduced and examined. Numerical characteristics are time-averaged in order to establish and trace out stable trends [9–11].

2. Synthesis and analysis of cell profiles. The time $t = t_0$ is fixed and the profiles $\boldsymbol{V}(t_0, z)$ are considered as functions of the altitude z, or the altitude $z = z_0$ is fixed and the strobes $\boldsymbol{V}(t, z_0)$ are considered as functions of time t. Mathematical models (regression lines) and confidence intervals on them are constructed. Time averaging was used in [9–11] to examine trends.

3. Synthesis and analysis of the two-dimensional distributions $\boldsymbol{V}(t,z)$. It is of significant interest to construct models of the fine structure of a wind stratum: structure functions, autocorrelations, regression lines of $\boldsymbol{V}(t,z)$ as functions of time t and altitude z.

In this paper we examine special features of the spatiotemporal dynamics of the wind velocity on the basis of real-time Doppler minisodar measurements and analyze and compare standard classical methods with methods based on robust nonparametric statistics.

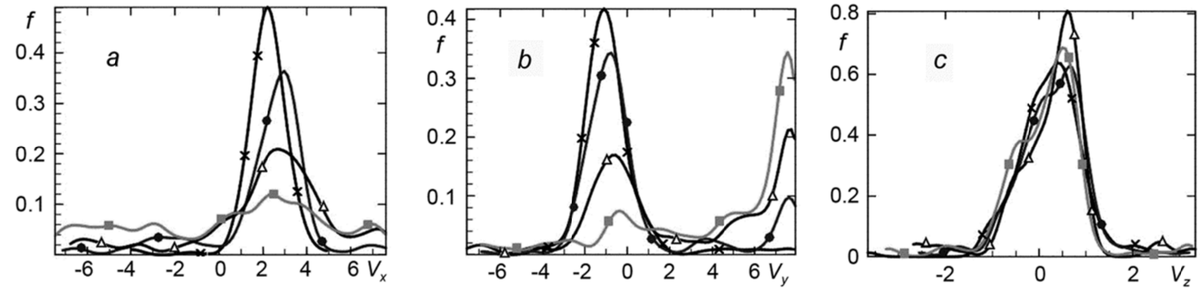

Fig. 1. Graphs of the density distributions of the *x*- (*a*), *y*- (*b*), and *z*-components (*c*) of the wind velocity for altitudes 50 (×), 100 (•), 150 (■), and 200 m (Δ).

2. ANALYSIS OF CELL ARRAY

We processed series of $N = 150$ profiles each over a 10-minute measurement period for the different components, altitudes, and times (cell array).

Let $\boldsymbol{v}_N = (v_1,...,v_N)$ be a sample of a the wind velocity component at the altitude *z* and time *t*, where $N = 150$ is the sample size. For each wind velocity component in the cell we constructed a graph of the estimate of the Rosenblatt–Parzen probability density of the form

$$f(v^z, h_N) = \frac{1}{Nh_N} \sum_{i=1}^{N} K\left(\frac{v^z - v_i^z}{h_N}\right), \tag{1}$$

where $K(u)$ is the kernel function and h_N is the width of the window [6]. As an example, Figure 1 displays graphs of the density distribution for three wind velocity components V_x, V_y, and V_z at fixed altitudes estimated from minisodar measurements taken on 13 October 2003 between 11:00 and 11:10 local time.

Even a simple visual analysis of the graphs enables one to draw a number of conclusions: the presence of outliers is more the rule than the exception; distributions are present both with *stretched* tails (*a*) and *light* tails (*c*); hardly any normal distributions were observed; the form of the marginal distributions varies strongly as a function of time of day of the observation. It should also be noted that for the *x*- and *y*-components the width of the distribution increases as the observation altitude is increased, and the maximum of the distribution function decreases, as was also noted in [2]. For the *y*-component we tracked the transition from a unimodal distribution to a bimodal one with increase of altitude. For the *z*-component the width of the distribution remains practically constant, but the maximum decreases with altitude.

Analysis of the marginal distributions shows that the problem belongs to the class of nonparametric problems of robust statistics [5, 6], which are characterized by the level of *a priori* uncertainty when the form of the distribution is unknown and there are deviations from the basic distribution, for example, in the form of outliers, asymmetry, etc. [6]. The parameters of position μ_n and scale of the wind field were calculated for the cells. Robust nonparametric estimates were found on the basis of the weighted maximum likelihood method (WMLM) [6, 7] by solving a system of equations of the form

TABLE 1. Characteristics of Estimates of μ_p and μ_n versus Altitude

Altitude, m	Parametric model (μ_p)			Nonparametric model (μ_n)			Efficiency
	Square of the bias	Variance	SD_p	Square of the bias	Variance	SD_n	
55	0.008143	0.000449	0.008593	0.006785	0.000890	0.007674	0.89
100	0.142441	0.000408	0.142849	0.010625	0.000921	0.011546	0.08
150	0.433752	0.000847	0.434599	0.001296	0.000396	0.001692	0.04
180	0.614029	0.001204	0.615233	0.012446	0.000699	0.013144	0.02

$$\begin{cases} \sum_{i=1}^{N} \tilde{f}_N^{\,l-1}(\nu_i^z, \mu_N, h_N \mid z) \sum_{j\neq i=1}^{N} K'(u_{ij}) = 0, \\ \sum_{i=1}^{N} \tilde{f}_N^{\,l}(v_i^z, \mu_N, h_N \mid z) \left(\frac{\sum_{\substack{j=1 \\ i\neq j}}^{N} K'\left(t_{ij}\right)\left(t_{i,j}\right) + K'\left(u_{ij}\right)\left(u_{ij}\right)}{2h_N \tilde{f}_N(v_i^z, \mu_N, h_N \mid z)} + \frac{1}{l+1} \right) = 0, \end{cases} \quad (2)$$

$$\tilde{f}_N(v^z, \mu, h_N \mid z) = \frac{1}{2Nh_N} \sum_{j=1}^{N} \left(K\left(\frac{v^z - v_j^z}{h_N} \right) + K\left(\frac{2\mu - v_j^z - v^z}{h_N} \right) \right),$$

$$K(u) = \frac{1}{\sqrt{2\pi}} e^{-\frac{u^2}{2}}, \; K'(u) = \frac{\partial}{\partial u} K(u), \; u_{ij} = \frac{2\mu_N - v_i^z - v_j^z}{h_N}, \; t_{ij} = \frac{v_i^z - v_j^z}{h_N}.$$

For comparison, we calculated the standard parametric estimates: the sample mean μ_p and the sample variance. Given the estimates μ_p and μ_n we found the biases, variances, standard deviations SD_p and SD_n by the bootstrap method – and determined the relative efficiency eff = SD_p/SD_n. As an example, Table 1 presents results of a comparison of μ_p and μ_n at different altitudes, and Fig. 2 displays the results of a comparison of the μ_p and μ_n profiles.

As follows from Table 1, the efficiency can vary significantly with altitude (from 2% to 89%). As can be seen from Fig. 2*a* and *b*, SD_p is mainly determined by the bias of the estimate, which can vary significantly both with altitude and with time. Figure 2*c* clearly shows such a dependence. On the basis of the bootstrap method, we determined the central confidence intervals of μ_p and μ_n from their profiles with a confidence level of 0.95. Table 2 presents calculated confidence intervals for a series of altitudes; Fig. 2*c* shows a plot of their corresponding profiles.

Analysis of Table 2 and Fig. 2*c* shows that widths of the confidence intervals $2\delta_p$ and $2\delta_n$ for μ_p and μ_n are of the same order of magnitude. At the same time, a significant bias of the estimate μ_p at altitudes greater than 70 m is clearly visible, which testifies to the presence of significant outliers at these altitudes.

TABLE 2. Confidence Intervals

Altitude, m	Parametric model (μ_p)		Nonparametric model (μ_n)	
	μ_p	δ_p	μ_n	δ_n
55	0.2402635	0.0357225	0.2302145	0.0452535
100	0.5648655	0.0327015	0.2907555	0.0473035
150	0.9759460	0.0476910	0.3533920	0.0348630
180	1.0202670	0.0578420	0.3460385	0.0407315

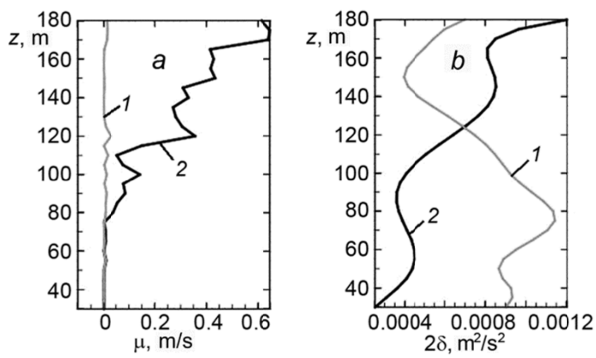

Fig. 2. Altitude dependence of characteristics of the estimates μ_n (curve *1*) and μ_p (curve *2*): *a*) square of the bias, *b*) variance, *c*) confidence intervals.

3. ANALYSIS OF ALTITUDE PROFILES AND TEMPORAL DYNAMICS OF WIND VELOCITY COMPONENTS

We fix the time $t = t_0$ and some averaging interval T. Let us consider the profiles $V(t_0, z)$ as functions of the altitude z. We processed series of 150 profiles over 10-minute measurement period (T = 10 min, sample size N = 5200) for the different components.

Let $\boldsymbol{v}_N^z = (v_1^z, ..., v_N^z)$ be a sample of the wind velocity components at the altitude $z_i = i \cdot 5,\ i = \overline{1, 40}$, where N = 5200 is the sample size. Let us consider the problem of constructing a mathematical model of the behavior of the profile $V(t_0, z)$. The given problem can be related to the problem of classical regression expressed in the form

$$v(z) = m(z) + \varepsilon , \tag{3}$$

where v is the the wind velocity component at the time t, $m(z)$ is the regression function, and ε is noise. We assume *a priori* that the random quantity ε has a probability density $f(\varepsilon)$ that is symmetric about zero, whose form, however, is unknown.

In [9, 11] a regression function in the form of a third-degree polynomial:

$$m_p(z) = \theta_0 + \theta_1 z + \theta_2 z^2 + \theta_3 z^3 \tag{4}$$

was used as a parametric model. Estimates of the parameters of model (4) were found using the method of least squares.

On the basis of the WMLM method [6], the parameters of local model (3) were estimated by solving a system of nonlinear equations of the form

TABLE 3. Average and Maximum Relative Efficiencies of Estimates

Measurement time, h:min	08:00–08:10	20:00–20:10
Average efficiency, %	38	3
Maximum efficiency, %	43	4

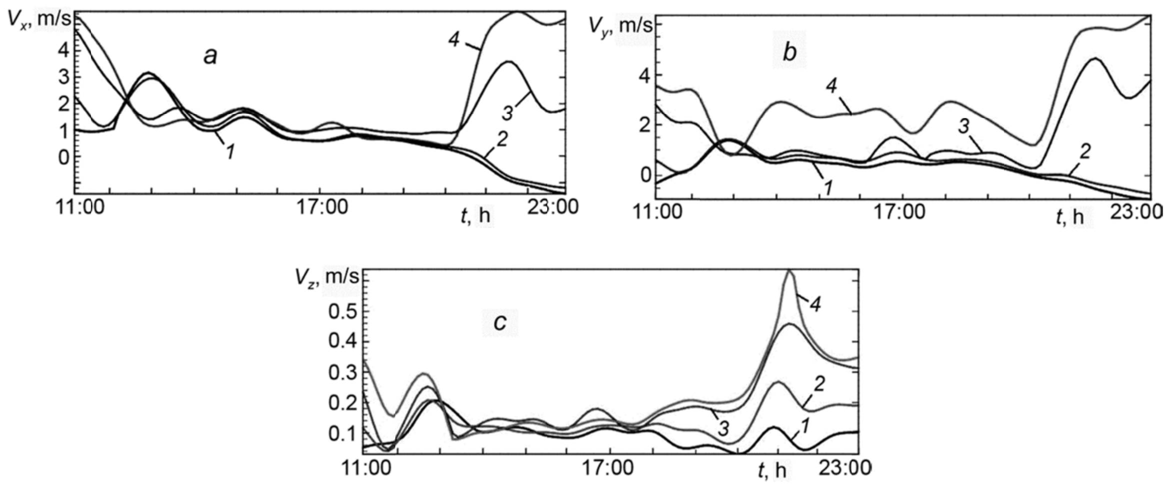

Fig. 3. Robust nonparametric estimates of the wind velocity plotted as functions of time for the altitudes 200 (curve *1*), 150 (curve *2*), 100 (curve *3*), and 50 m (curve *4*).

$$\sum_{i=1}^{N} \tilde{f}_2^{l-1}(v_i, m_n) K_1\left(\frac{z - z_i}{h_{1N}}\right) \sum_{\substack{j=1 \\ i \neq j}}^{N} K_2'\left(w_{i,j}\right) K_1\left(\frac{z - z_j}{h_{1N}}\right) = 0\,,$$

$$\sum_{i=1}^{N} \tilde{f}_2^{l}(v_i, \mu_n) K_1\left(\frac{z - z_i}{h_{1N}}\right) \sum_{\substack{j=1 \\ i \neq j}}^{N} K_1\left(\frac{z - z_j}{h_{1N}}\right)$$
$$\times\left(1 + \left[2N(1+l) h_{2N} \cdot \tilde{f}_2(v_i, m_n)\right]^{-1} \sum\nolimits_{j=1}^{N} \left(K_2'\left(u_{i,j}\right) u_{i,j} + K_2'\left(w_{i,j}\right) w_{i,j}\right)\right) = 0, \qquad (5)$$

$$\tilde{f}_2(v_i^z, \mu_n) = \frac{1}{2N \cdot h_{2N}} \sum\nolimits_{j=1}^{N} \left(K_2\left(\frac{v_i^z - v_j^z}{h_{2N}}\right) + K_2\left(\frac{2m_n - v_i^z - v_j^z}{h_{2N}}\right) \right),$$

$$K'(x) = \frac{\partial}{\partial x} K(x)\,,\ u_{i,j} = \frac{v_i^z - v_j^z}{h_{2N}}\,,\ w_{i,j} = \frac{2m_n - v_i^z - v_j^z}{h_{2N}}\,.$$

By way of an example, Fig. 2*c* displays a graph of the regression lines and their confidence intervals. Table 3 lists the mean values and maximum relative efficiencies of the parametric estimate expressed as a ratio to the nonparametric estimate over their profiles in the morning and evening hours.

In analogy with the construction of the mathematical robust nonparametric model of profiles (5), robust nonparametric regressions were constructed for the the wind velocity components on the basis of minisodar measurements conducted from 11:00 to 23:00 on 13 September (Fig. 3), which characterize their hourly semidiurnal spatiotemporal dynamics. All three components have maxima in the morning and evening hours. The maxima in the evening hours for the *y*- and *z*-components are more strongly expressed than the maxima in the morning hours. For the *x*- and *y*-components (Fig. 3*a* and *b*) the shear was closely tracked in the evening hours (from 20:00 to 23:00). At these times V_x varies from 5.2 m/s at an altitude of 50 m to –1.4 m/s at an altitude of 200 m, and V_y varies from 6.5 to –1 m/s.

The obtained results allow us to draw the following conclusions:

1. Analysis of the hourly semidiurnal dynamics showed that all three wind velocity components have maxima in the morning and evening hours. For the *y*- and *z*-components, the maxima in the evening hours are more strongly expressed than in the morning hours. For the *x*- and *y*-components the wind shear was closely tracked in the evening hours.

2. We obtained the distribution law for each wind velocity component. We found that for the *x*- and *y*-components the width of the distribution increases as the observation altitude is increased, and the maximum of the distribution function decreases, which is in agreement with the data available in the literature. For the *y*-component a transition from a unimodal to a bimodal distribution with increasing altitude is traced out. For the *z*-component the width of the distribution remains practically constant but the maximum decreases with altitude.

3. The efficiency of classical data processing methods in comparison with robust nonparametric methods can be extraordinarily low, in a number of cases reaching as low as ≈5% (Tables 1 and 3).

4. The presence of different kinds of outliers (Fig. 1) leads to extremely unstable behavior of the SD_p. At the same time, the robust nonparametric estimates are stable to outliers (Table 1). As this work has shown, this is due to the appearance of significant biases of the classical estimates (Fig. 2 and Table 1).

5. The use of nonparametric methods makes it possible to obtain data that cannot be obtained by conventional methods.

REFERENCES

1. N. P. Krasnenko, Acoustic Sounding of the Atmospheric Boundary Layer [in Russian], Vodolei, Tomsk (2001).
2. S. Breadly, Atmospheric Acoustic Remote Sensing. Principles and Applications, CRC Press Taylor & Francis Group, Boca Raton, Florida (2007).
3. A. B. Rykhlov, Climatological estimate of the wind-energy potential at different altitudes (in the Example of Southwestern Russia), Author's Abstract of Doct. Geograph. Sci. Dissert., Kazan, Russia (2012).
4. P. J. Huber and E. M. Ronchetti, Robust Statistics, John Wiley & Sons, New York (2009).
5. V. A. Simakhin, Robust Nonparametric Estimates, Lambert Academic Publishing, Saarbrücken, Germany (2011).
6. V. A. Simakhin and O. S. Cherepanov, Int. J. Innovat. Comput. Inform. Control, **487**, 397–405 (2014).
7. V. A. Simakhin and O. S. Cherepanov, Proceedings of the XXth International Symposium "Optics of the Atmosphere and Ocean. Atmospheric Physics" [in Russian] [Electronic resource], Izd. IOA SB RAS, Tomsk (2014), pp. 277–281.
8. http://minisodar.org.
9. N. P. Krasnenko, M. V. Tarasenkov, and L. G. Shamanaeva, Russ. Phys. J., **57**, No. 11, 1539–1546 (2014).
10. O. F. Kapegesheva, N. P. Krasnenko, and L. G. Shamanaeva, Proc. SPIE. 20th International Symposium on Atmospheric and Ocean Optics: Atmospheric Physics, 92924N (November 25, 2014); Vol. 9292, doi: 10.1117/12.2075651 (6 pp.).
11. O. F. Kapegesheva, N. P. Krasnenko, and L. G. Shamanaeva, Proceedings of the XXth International Symposium "Optics of the Atmosphere and Ocean. Atmospheric Physics" [in Russian] [Electronic resource], Izd. IOA SB RAS, Tomsk (2014), pp. D118–D121. CD-ROM.